Improved stability regions for ground states of the extended Hubbard model

Zsolt Szabó*
Institut für Theoretische Physik, Universität zu Köln, Zülpicher Strasse 77, D-50937 Köln, Germany
(Received 29 June 1998; revised manuscript received 16 November 1998)

The ground-state phase diagram of the extended Hubbard model containing nearest- and next-to-nearest-neighbor interactions is investigated in the thermodynamic limit using an exact method. It is found that taking into account local correlations and adding next-to-nearest-neighbor interactions both have significant effects on the position of the phase boundaries. Improved stability domains for the η-pairing state and for the fully saturated ferromagnetic state at half-filling have been constructed. The results show that these states are the ground states for model Hamiltonians with realistic values of the interaction parameters. [S0163-1829(99)12015-0]

I. INTRODUCTION

Exact solutions in physics are of great importance, since in some cases the errors introduced by the approximations may dominate the results to such an extent that one might end up with an incorrect description of the studied phenomenon. When applying an analytic, but nonexact, approach one has to know to what extent the approximation is valid. In case of perturbative methods a well-defined *small* parameter can ensure that the higher-order terms are indeed negligible. Often, it is hard to find such a small parameter due to the fact that the given phenomenon itself has strong-coupling characteristics, i.e., the associated correlation effects are not small at all. This is especially true by the investigation of strongly correlated electron systems. Ferromagnetism is an example for the *intermediate-to-strong* coupling phenomenon, where one has to be very cautious to apply perturbative approaches.

Considering the exact results with respect to the dimensionality D, we can see that most of them have been derived in two limiting cases: either $D=1$ or $D=\infty$. For example, the exact solution of the Hubbard model was given in $D=1$ dimension by means of the Bethe ansatz by Lieb and Wu.[1] The other class of exact solutions belongs to the other limiting case, i.e., $D=\infty$, when the dynamical mean-field approximation becomes exact.[2,3] The situation, however, gets more complicated as physically interesting, lower-dimensional cases (e.g., systems in $D=2$ or $D=3$ dimensions) are considered. $D>1$ rules out the applicability of the well-established Bethe-ansatz approach, while mean-field-like descriptions lead to qualitatively or quantitatively incorrect conclusions, because the effects of spatial fluctuations are not taken properly into account.[4,5]

In recent years, some exact, *nonperturbative* methods have been developed to investigate the ground state of Hubbard and Hubbard-like models in large parameter regimes.[6–13] In the present work we focus on the so-called optimum ground-state method (OGS) established by de Boer and Schadschneider.[12] Using this method one can obtain rigorous constraints on the model parameters which define regions where, e.g., the charge-density wave, the Néel, the fully saturated ferromagnetic, or the η-pairing state of momentum P becomes the exact ground state of the Hamiltonian.

The basic idea of the OGS method is to diagonalize a specially chosen local Hamiltonian and to tune all the model parameters in such a way that all local eigenstates that are needed to the construction of a given global ground state are also local ground states. This means that, on one hand, the corresponding eigenvalues of the local Hamiltonians should be all equal in magnitude and, on the other hand, this common value should be the lowest eigenvalue of the local problem. Following this method, one can obtain different regions in the parameter space of the model defined by inequalities. These inequalities mean *sufficient* conditions for a state to be the ground state inside a special region. Outside the derived region the state under study may or may not be the ground state of the model.

There are basically two different ways to enlarge the region of guaranteed stability: taking a larger local Hamiltonian or incorporating next-to-nearest-neighbor interactions. As far as the first approach is concerned, it is obvious that the extent of local correlations that are taken into account is controlled by the size of the local Hamiltonian to be diagonalized exactly. Therefore, using local Hamiltonians defined on larger clusters of the lattice should typically lead to better constraints (i.e., extended stability regions), even if purely nearest-neighbor interactions are present.

It is also well known that next-to-nearest-neighbor hopping has important effects. For instance, it was shown rigorously by Tasaki[14] that the pure Hubbard model characterized by hopping of electrons between nearest- and next-to-nearest-neighboring sites with dispersive bands exhibits ferromagnetism for finite Coulomb interaction at zero temperature. Recent projection quantum Monte Carlo studies by Hlubina, Sorella, and Guinea[15] confirmed this fact for finite temperatures, too. Beside the consequences of longer-range hopping, the importance of nearest and next-to-nearest-neighbor off-site interactions (both diagonal and off-diagonal) has also been emphasized both from experimental[16] and from theoretical[4,10,11,17,18] sides. These extra terms (density-density type interaction, correlated hopping of electrons, hopping of electron pairs, and the exchange coupling) all originate from the spin-independent Coulomb interaction of electrons. Nevertheless, the values of

these longer-range interactions (e.g., between next-to-nearest-neighboring sites) are known neither theoretically nor experimentally because of the complicated nature of screening processes in solids. However, it is obvious that these interactions are present in real materials. Their strength decreases with increasing interatomic distances on the lattice and they can have important effects on the characteristics of strongly correlated electron systems. Hence, it is a challenging task to incorporate and to treat them in an exact way on the level of the model Hamiltonian.

The aim of the present paper is twofold. First, we would like to extend the previous calculations of Ref. 12 by choosing a larger local Hamiltonian that is defined on elementary plaquettes consisting of four lattice sites of the D-dimensional hypercubic lattice. Using these local Hamiltonians and a simple, numerically exact method we have constructed the stability domains for the η-pairing states of momentum $P=0,\pi$ and for the fully saturated ferromagnetic state in the parameter space of an extended Hubbard model with a half-filled band. Given the size of the local Hamiltonian, the diagonalization is done numerically. The stability regions are deduced from the equality of the lowest eigenvalue of the chosen local Hamiltonian and of an upper bound derived appropriately from the variational principle of quantum mechanics. Second, the present choice of the larger local Hamiltonian gives us a simple way to incorporate next-to-nearest-neighbor interactions, to treat them exactly, and to investigate their effects on stability.

The paper is organized as follows: in Sec. II we introduce the method. In Sec. III the global Hamiltonian and the corresponding local Hamiltonian are defined. Sections IV A and IV B contain the stability domains in $D=2,3$ for the η-pairing states of momentum P and for the fully saturated ferromagnetic case, respectively. Finally a short summary and discussion closes the presentation in Sec. V.

II. METHOD

Let us consider a model Hamiltonian defined on a discrete lattice. This (so-called global) Hamiltonian can be decomposed into the sum of equivalent local Hamiltonians h_{cluster} defined on identical clusters of lattice sites, the union of which covers the lattice. In other words,

$$H=\sum_{\text{all clusters}} h_{\text{cluster}}. \tag{1}$$

If only on-site interactions are considered, each cluster might consist of a single lattice point and h_{cluster} is simply a Hamiltonian defined on the individual lattice points. If intersite interactions are also present, the cluster has to consist of (at least) two lattice sites (in case of only nearest-neighbor interactions) and the proper *minimal* local Hamiltonian is actually a Hamiltonian defined on a bond joining two (in the simplest case nearest neighboring) sites. Nevertheless, the incorporation of longer and longer range interactions, or of more and more spatial correlations, requires the enlargement of the minimal cluster and hence the corresponding local Hamiltonian h_{cluster}. In principle, even infinite-range interactions and correlations can be taken into account, but this would require $h_{\text{cluster}}=H$. The tractable cluster size is, however, limited by the feasibility of the necessary exact diagonalizations.

Setting up the local Hamiltonian and choosing a suitable local basis, the eigenvalue problem

$$h_{\text{cluster}}|\phi_{\text{cluster}}\rangle=\epsilon_{\text{cluster}}|\phi_{\text{cluster}}\rangle \tag{2}$$

can be solved exactly. Thus the full spectrum $\epsilon^{i}_{\text{cluster}}$ ($i=1,\ldots,\dim(h_{\text{cluster}})$) of h_{cluster} can be obtained. Since the clusters of decomposition are equivalent, the exact ground-state energy E_{GS} is bounded from below by the relation

$$E_{\text{lower}}=N_{\text{cluster}}\min_{i}\epsilon^{i}_{\text{cluster}}\leqslant E_{\text{GS}}, \tag{3}$$

where the number of clusters on the considered lattice can be written as $N_{\text{cluster}}=fL$. Here f represents a simple combinatorical factor depending on the dimension and structure of the underlying lattice and L stands for the number of lattice sites.

The variational principle of quantum mechanics provides an upper bound for E_{GS}, namely,

$$E_{\text{GS}}\leqslant\frac{\langle\Psi_{\text{trial}}|H|\Psi_{\text{trial}}\rangle}{\langle\Psi_{\text{trial}}|\Psi_{\text{trial}}\rangle}=E_{\text{upper}}, \tag{4}$$

where $|\Psi_{\text{trial}}\rangle$ stands for an arbitrary trial wave function. In our case $|\Psi_{\text{trial}}\rangle$ is an exact eigenstate of the global Hamiltonian for a certain set of model parameters.

Combining now Eqs. (3) and (4) yields

$$E_{\text{lower}}\leqslant E_{\text{GS}}\leqslant E_{\text{upper}}. \tag{5}$$

Exploiting that both E_{lower} and E_{upper} are analytic functions of the couplings of the global Hamiltonian, after carefully adjusting the coupling constants one can satisfy the equality

$$E_{\text{lower}}=E_{\text{upper}}\equiv E_{\text{GS}}, \tag{6}$$

which means that for a certain set of model parameters (in a special sector of the ground-state phase diagram) the exact ground-state energy E_{GS} is found. Furthermore, if the ground state has no degeneracy, the exact ground state $|\Psi_{\text{GS}}\rangle$ of the global Hamiltonian is also found. In our case the nondegeneracy is provided by the fact that the states we consider (see Sec. IV) can be built up simply by using the lowest-energy eigenstate of the local Hamiltonian. As an example let us consider the case of the $D=1$-dimensional half-filled chain with bonds as clusters. For certain values of the coupling constants it can be concluded that the nondegenerate lowest eigenvalue of the local Hamiltonian belongs to the parallel orientation of spins included on the bond. Since the bonds are equivalent, all the bonds along the chain contain parallel-oriented spins with the same local energy for the given set of model parameters. This fact yields the long-range order of spins (here ferromagnetism) and also the nondegeneracy of the global ground state (apart from the spin degeneracy). Similar arguments hold for the nondegeneracy of the ground state in higher dimensions, too.

Changing now the trial wave function and following the procedure discussed above a new ground state in a different region of the phase diagram can be found. Furthermore, re-

peating the method with more and more trial wave functions a large portion of the ground-state phase diagram of the model can be explored.

III. GLOBAL AND LOCAL HAMILTONIAN

Let us define now our global Hamiltonian on a D-dimensional hypercubic lattice ($D>1$) in the following form:

$$H_{\rm glob}=U\hat{U}+\sum_{i,j}\left[-t_{ij}\hat{t}_{ij}+X_{ij}\hat{X}_{ij}+V_{ij}\hat{V}_{ij}+Y_{ij}\hat{Y}_{ij}+J_{ij}\hat{J}_{ij}\right]-\mu\hat{\mu}, \tag{7}$$

where

$$\hat{U}=\sum_i n_{i\uparrow}n_{i\downarrow},$$

$$\hat{t}_{ij}=\sum_\sigma c^\dagger_{i\sigma}c_{j\sigma},$$

$$\hat{X}_{ij}=\sum_\sigma c^\dagger_{i\sigma}c_{j\sigma}(n_{i,-\sigma}+n_{j,-\sigma}),$$

$$\hat{V}_{ij}=\tfrac{1}{2}\sum_{\sigma,\sigma'} n_{i\sigma}n_{j\sigma'},$$

$$\hat{Y}_{ij}=c^\dagger_{i\uparrow}c^\dagger_{i\downarrow}c_{j\downarrow}c_{j\uparrow},$$

$$\hat{J}_{ij}=\tfrac{1}{2}\Delta^{XY}_{ij}(S_i^+S_j^-+S_j^+S_i^-)+\Delta^Z_{ij}S^z_iS^z_j,$$

$$\hat{\mu}=\sum_{i,\sigma} n_{i\sigma}.$$

Here the fermion operators $c^\dagger_{i\sigma}$ ($c_{i\sigma}$) create (annihilate) electrons with spin σ in the single tight-binding Wannier orbital associated with site i. $n_{i\sigma}$ is the particle number operator of electrons with spin σ, and $n_i=n_{i\uparrow}+n_{i\downarrow}$. Furthermore, the spin operators are given by $S_i^+=c^\dagger_{i\uparrow}c_{i\downarrow}$, $S_i^-=c^\dagger_{i\downarrow}c_{i\uparrow}$, and $S_i^z=\frac{1}{2}(n_{i\uparrow}-n_{i\downarrow})$. The above Hamiltonian contains a term corresponding to the familiar Hubbard term of doubly occupied sites (U), the hopping of a single electron (characterized by t_{ij}), a density dependent (or correlated) hopping term (X_{ij}), an intersite density-density type interaction of electrons (V_{ij}), a term describing the hopping of electron pairs (Y_{ij}), for $\Delta^{XY}_{ij}=\Delta^Z_{ij}=1$ a Heisenberg-type exchange interaction of spins (J_{ij}), and a chemical potential term (μ). We note that $\Delta^{XY}_{ij}=0$ and $\Delta^Z_{ij}=1$ represents an Ising-type coupling of electron spins, while the case of $\Delta^{XY}_{ij}=1$ and $\Delta^Z_{ij}=0$ corresponds to an XY-type interaction. $J_{ij}>0$ ($J_{ij}<0$) means antiferromagnetic (ferromagnetic) type of exchange. The relevance of the present model for real materials is discussed, e.g., in Refs. 4 and 20.

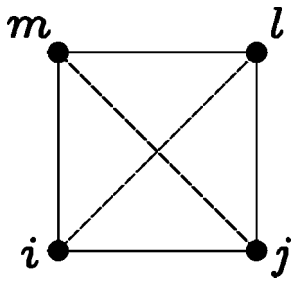

FIG. 1. An elementary plaquette of the $D=2$-dimensional square lattice. Solid lines represent different types of nearest-neighbor couplings while dashed lines symbolize the next-to-nearest-neighbor ones. The local Hamiltonian is defined on this cluster.

In the rest of the paper we investigate only couplings between on-site, nearest-neighbor, and next-to-nearest-neighbor electrons. Incorporating this restriction into Eq. (7) and using the convention $A_l=A_{ij}$ ($l=1,2$ for i, j being nearest- and next-to-nearest-neighboring sites, respectively) for the intersite couplings, one can rewrite the global Hamiltonian as

$$\begin{aligned}H_{\rm glob}=&U\sum_{i=1}^{L}(n_{i\uparrow}-\tfrac{1}{2})(n_{i\downarrow}-\tfrac{1}{2})+\sum_{l=1}^{2}\sum_{\langle ij\rangle_l}\\&\times\Bigg\{\tfrac{1}{2}\sum_\sigma\left[X_l(n_{i,-\sigma}+n_{j,-\sigma})-t_l\right](c^\dagger_{i\sigma}c_{j\sigma}+c^\dagger_{j\sigma}c_{i\sigma})\\&+\tfrac{1}{2}V_l(n_i-1)(n_j-1)+\tfrac{1}{2}Y_l(c^\dagger_{i\uparrow}c^\dagger_{i\downarrow}c_{j\downarrow}c_{j\uparrow}\\&+c^\dagger_{j\uparrow}c^\dagger_{j\downarrow}c_{i\downarrow}c_{i\uparrow})+\tfrac{1}{2}J^{(l)}_{\rm xy}(S_i^+S_j^-+S_j^+S_i^-)+J^{(l)}_{\rm z}S^z_iS^z_j\Bigg\}\\&-\mu\hat{\mu}-E_0.\end{aligned} \tag{8}$$

Here $\Sigma_{\langle ij\rangle_l}$ means a summation over nearest-neighboring ($l=1$) and next-to-nearest neighboring ($l=2$) sites. The new notations $J^{(l)}_{\rm xy}=\Delta^{XY}_lJ_l$ and $J^{(l)}_{\rm z}=\Delta^Z_lJ_l$ are also used. In the special case of $\Delta^{XY}_l=\Delta^Z_l=1$, however, the $J_l\equiv J^{(l)}_{\rm xy}=J^{(l)}_{\rm z}$ notation will be kept for the sake of clarity. E_0 represents a numerical constant that shifts the zero point of the energy scale. We remark that during the reformulation of Eq. (7) to Eq. (8) the chemical potential is also shifted by some constant.

Because we have only nearest- and next-to-nearest-neighbor interactions, the fully symmetric minimal clusters are the two-dimensional elementary plaquettes of the $D=2$-dimensional square lattice, as depicted in Fig. 1. All $D>2$-dimensional hypercubic lattices can be covered with the elementary plaquettes; however, in those cases the D-dimensional hypercubes would be the fully symmetric minimal clusters.

Following the method of Sec. II the global Hamiltonian can be rewritten in terms of such plaquettes ($\Sigma_{[i,j,l,m]}$ means a summation over the plaquettes) as

$$H_{\rm glob}=\sum_{[i,j,l,m]}h_{ijlm} \tag{9}$$

with

$$h_{ijlm}=\frac{U}{z_2}\sum_{\alpha\in\mathcal{A}_0}(n_{\alpha\uparrow}-\tfrac{1}{2})(n_{\alpha\downarrow}-\tfrac{1}{2})+\frac{X_1}{4f_1}\sum_{(\alpha,\beta)\in\mathcal{A}_N}\sum_{\sigma}(c^{\dagger}_{\alpha,\sigma}c_{\beta,\sigma}+c^{\dagger}_{\beta,\sigma}c_{\alpha,\sigma})(n_{\alpha,-\sigma}+n_{\beta,-\sigma})$$
$$+\frac{X_2}{f_2}\sum_{(\alpha,\beta)\in\mathcal{A}_{NN}}\sum_{\sigma}(c^{\dagger}_{\alpha,\sigma}c_{\beta,\sigma}+c^{\dagger}_{\beta,\sigma}c_{\alpha,\sigma})(n_{\alpha,-\sigma}+n_{\beta,-\sigma})-\frac{t_1}{4f_1}\sum_{(\alpha,\beta)\in\mathcal{A}_N}\sum_{\sigma}(c^{\dagger}_{\alpha,\sigma}c_{\beta,\sigma}+c^{\dagger}_{\beta,\sigma}c_{\alpha,\sigma})$$
$$-\frac{t_2}{f_2}\sum_{(\alpha,\beta)\in\mathcal{A}_{NN}}\sum_{\sigma}(c^{\dagger}_{\alpha,\sigma}c_{\beta,\sigma}+c^{\dagger}_{\beta,\sigma}c_{\alpha,\sigma})+\frac{V_1}{4f_1}\sum_{(\alpha,\beta)\in\mathcal{A}_N}(n_\alpha-1)(n_\beta-1)+\frac{V_2}{f_2}\sum_{(\alpha,\beta)\in\mathcal{A}_{NN}}(n_\alpha-1)(n_\beta-1)$$
$$+\frac{Y_1}{4f_1}\sum_{(\alpha,\beta)\in\mathcal{A}_N}(c^{\dagger}_{\alpha\uparrow}c^{\dagger}_{\alpha\downarrow}c_{\beta\downarrow}c_{\beta\uparrow}+c^{\dagger}_{\beta\uparrow}c^{\dagger}_{\beta\downarrow}c_{\alpha\downarrow}c_{\alpha\uparrow})+\frac{Y_2}{f_2}\sum_{(\alpha,\beta)\in\mathcal{A}_{NN}}(c^{\dagger}_{\alpha\uparrow}c^{\dagger}_{\alpha\downarrow}c_{\beta\downarrow}c_{\beta\uparrow}+c^{\dagger}_{\beta\uparrow}c^{\dagger}_{\beta\downarrow}c_{\alpha\downarrow}c_{\alpha\uparrow})$$
$$+\frac{J^{(1)}_{xy}}{4f_1}\sum_{(\alpha,\beta)\in\mathcal{A}_N}(S^{+}_{\alpha}S^{-}_{\beta}+S^{+}_{\beta}S^{-}_{\alpha})+\frac{J^{(2)}_{xy}}{f_2}\sum_{(\alpha,\beta)\in\mathcal{A}_{NN}}(S^{+}_{\alpha}S^{-}_{\beta}+S^{+}_{\beta}S^{-}_{\alpha})+\frac{J^{(1)}_{z}}{2f_1}\sum_{(\alpha,\beta)\in\mathcal{A}_N}S^{z}_{\alpha}S^{z}_{\beta}+J^{(2)}_{z}\sum_{(\alpha,\beta)\in\mathcal{A}_{NN}}S^{z}_{\alpha}S^{z}_{\beta}$$
$$-\frac{\mu}{z_2}\sum_{\alpha\in\mathcal{A}_0}n_\alpha. \tag{10}$$

Here $f_1=z_2/z_1$ and $f_2=2$ are numerical constants [$z_1=2D$ and $z_2=4\binom{D}{2}$ are the number of nearest- and next-to-nearest-neighboring sites, respectively, on the D-dimensional hypercubic lattice]. They are needed to avoid double or higher counting of intersite interactions during the plaquette summation. Furthermore, t_1,X_1,V_1,Y_1 are the values of single-electron hopping, correlated hopping, density-density type interaction, and pair-hopping between nearest neighboring sites, respectively, while t_2,X_2,V_2,Y_2 indicate the analogous processes between next-to-nearest-neighboring sites. U is the Hubbard interaction that can either be positive or negative in our model. To mimic real systems, however, it should be repulsive. In addition, spin interactions with exchange couplings $J^{(1)}_{xy}$, $J^{(2)}_{xy}$, $J^{(1)}_{z}$, and $J^{(2)}_{z}$ are included on the plaquette. Further notations: $\mathcal{A}_0=\{i,j,l,m\}$ means the set of individual lattice points, $\mathcal{A}_N=\{(i,j),(j,l),(l,m),(m,i)\}$ represents the set of nearest-neighboring sites, and $\mathcal{A}_{NN}=\{(i,l),(j,m)\}$ indicates the set of next-to-nearest-neighboring sites on the plaquette (see Fig. 1). The possibility of anisotropies can be naturally incorporated into the local (and also global) Hamiltonian via the nonequivalence of the orthogonal directions of the plaquette. The effects, however, are not discussed in the present paper.

To apply Eq. (6) the connection between the number of lattice sites L and the number of clusters N_{cluster} (here plaquettes) is also needed. Combinatoric considerations give the following simple result for this quantity on a D-dimensional hypercubic lattice,

$$N_{\text{cluster}}=\tfrac{1}{2}D(D-1)L. \tag{11}$$

IV. RESULTS

As an illustration of the method described in Sec. II we consider a few physically interesting states, the η-pairing states of momentum P (Sec. IV A), which show off-diagonal long-range order and are hence superconducting, and the fully saturated ferromagnetic state (Sec. IV B). We determine under what conditions these states are the ground states of the global Hamiltonian H_{glob}. All the calculations presented are done at half-filling. Except the η-pairing state of momentum $P=0$, it is not possible to express the results in a compact analytic form as has been done earlier in Ref. 12. Therefore, and for the sake of visualization, we have restricted ourselves to special cuts of the parameter space in illustrating the effects of the larger local Hamiltonians and of next-to-nearest-neighbor couplings. The cuts are chosen in such a way that the corresponding ground-state phase diagrams can easily be compared with the previously published rigorous results of Strack and Vollhardt,[11] de Boer and co-workers,[12,21] and Montorsi and Campbell.[22] In principle, one can also investigate the role of each nearest- and next-to-nearest-neighbor interactions separately, one by one, using our method.

A. η-pairing states of momentum P

The definition of the η-pairing operator of momentum P is given by the relation

$$\eta^{\dagger}_{\text{P}}=\sum_{j=1}^{L}e^{iPj}c^{\dagger}_{j\downarrow}c^{\dagger}_{j\uparrow}. \tag{12}$$

Using this operator an η-pairing state of momentum P and of pairs N can be constructed as

$$|\Psi_\eta(\text{N,P})\rangle=K(\eta^{\dagger}_{\text{P}})^N|0\rangle, \tag{13}$$

where $K=\{[(L-N)!]/L!N!\}^{1/2}$ is a normalization factor. For further details about the η-pairing states the reader is referred to the literature.[21–25] Since we would like the η-pairing states to be the ground state of our model, it is instructive to calculate the commutator of the η operator with the global Hamiltonian H_{glob}. One finds that

$$[H,\eta^{\dagger}_{\text{P}}]=\sum_{k=1}^{2}\Bigg[\tfrac{1}{2}(X_k-t_k)\sum_{\langle jl\rangle_k}(e^{iPj}+e^{iPl})(c^{\dagger}_{j\downarrow}c^{\dagger}_{l\uparrow}+c^{\dagger}_{l\downarrow}c^{\dagger}_{j\uparrow})$$
$$+\tfrac{1}{2}X_k\sum_{\langle jl\rangle_k}(e^{iPj}-e^{iPl})$$
$$\times[(n_{l\uparrow}-n_{j\downarrow})c^{\dagger}_{l\downarrow}c^{\dagger}_{j\uparrow}+(n_{l\downarrow}-n_{j\uparrow})c^{\dagger}_{j\downarrow}c^{\dagger}_{l\uparrow}]$$

$$+\sum_{\langle jl\rangle_k}\{(\tfrac{1}{2}Y_k e^{iPj}-U_k e^{iPl})(n_j-1)c^\dagger_{l\uparrow}c^\dagger_{l\downarrow}$$

$$+(\tfrac{1}{2}Y_k e^{iPl}-U_k e^{iPj})(n_l-1)c^\dagger_{j\uparrow}c^\dagger_{j\downarrow}\}\Big]-2\mu\eta^\dagger_{\mathrm{P}}. \tag{14}$$

Calculating now the quantity $[H_{\mathrm{glob}},(\eta^\dagger_{\mathrm{P}})^N]|0\rangle$, one can easily deduce the parameters where the η-pairing states of momentum P are the ground state of the starting model; for momentum $P=0$ one arrives at the requirements $X_i=t_i$ and $Y_i=2V_i$ $(i=1,2)$, while for momentum $P=\pi$ the conditions $X_2=t_2$ and $Y_i=(-1)^i 2V_i$ $(i=1,2)$ must be satisfied. One would also look for η-pairing states of momentum $P\neq 0$ or $P\neq\pi$. These, however, represent the ground states of the global Hamiltonian in Eq. (7), where $X_i=t_i$ $(i=1,2)$, $U\leqslant -4t_1$ and all the other interaction constants are zero.[26,27]

Using the η-pairing states as trial wave functions, the upper bound in the thermodynamic limit for the ground-state energy per lattice site L is

$$\frac{E^{\eta_{\mathrm{P}}}_{\mathrm{upper}}}{L}=\tfrac{1}{4}(U+z_1V_1+z_2V_2)+\tfrac{1}{2}n(\tfrac{1}{2}n-1)$$

$$\times\sum_{l=1}^{2}z_lV_l+\tfrac{1}{4}n(1-\tfrac{1}{2}n)\sum_{l=1}^{2}z_lY_l\cos^lP-\mu n. \tag{15}$$

Exploiting the constraints between the amplitudes of pair-hopping Y_i and that of density-density type interaction V_i one gets for the half-filled case $(n=1)$ that

$$E^{\eta_{\mathrm{P}}}_{\mathrm{upper}}=\tfrac{1}{4}L\left(U+\sum_{l=1}^{2}z_lV_l\right)-\mu L. \tag{16}$$

Despite the fact that the upper bounds for the η-pairing states of momentum $P=0$ and $P=\pi$ are identical, there is a characteristic difference between the two sets of wave functions; the state $|\Psi_\eta(\mathrm{N},\mathrm{P}=\pi)\rangle$ remains an exact eigenstate of the global Hamiltonian H_{glob} even if $X_1\neq t_1$.

As mentioned earlier, it is possible to include more spatial correlations using local Hamiltonians defined on larger clusters of the lattice. This leads to the extension of the stability of the chosen state and means an improvement on the phase boundaries. For the η-pairing state of momentum $P=0$ this effect is depicted in Fig. 2, where the $\tilde{J}_{\mathrm{xy}}$-$\tilde{J}_{\mathrm{z}}$ cut of the coupling constants' space is chosen. The inner triangle corresponds to the stability domain of the η_0-state determined by the OGS method of de Boer and Schadschneider[12] using bond Hamiltonians with purely nearest-neighbor interactions. The shaded regions give the improvements of the boundaries applying our method with plaquette Hamiltonians containing only nearest-neighbor interactions. The axes $\tilde{J}_{\mathrm{a}}=J^{(1)}_{\mathrm{a}}A(U,V_1)$ (a=xy,z) represent the rescaled values of nearest-neighbor exchange interactions with the scaling factor of

$$A(U,V_1)=\left[2\left|\frac{2U}{z_1}+V_1\right|\right]^{-1}. \tag{17}$$

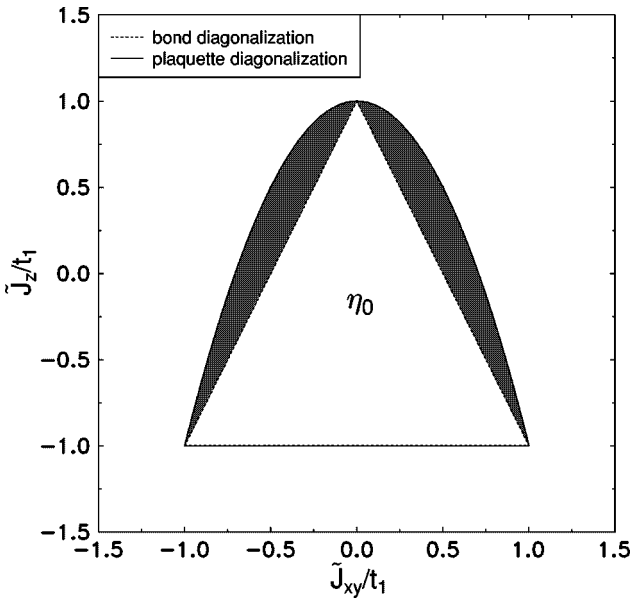

FIG. 2. Exact stability region of η-pairing state of momentum $P=0$ (η_0) at half-filling. The shaded region represents the enlargement of the stability domain due to the choice of local Hamiltonian defined on elementary plaquettes (see Fig. 1) of the lattice. All the next-to-nearest-neighbor interactions are kept zero.

From Fig. 2 one can immediately read off the stability criteria for the η_0 state to be the ground state of H_{glob}. In the absence of next-to-nearest-neighbor interactions (i.e., $t_2=X_2=V_2=Y_2=J_2=0$) for $V_1\leqslant 0$ values of nearest-neighbor density-density type interaction

$$V_1\leqslant 0,$$

$$-1\leqslant\frac{\tilde{J}_{\mathrm{z}}}{t_1}\leqslant -2\left(\frac{\tilde{J}_{\mathrm{xy}}}{t_1}\right)^2+1. \tag{18}$$

This is a considerable improvement over the $V_1\leqslant 0$, $-1\leqslant\tilde{J}_{\mathrm{z}}/t_1\leqslant -2|\tilde{J}_{\mathrm{xy}}/t_1|+1$ criteria derived following Ref. 12 using bond Hamiltonians.

If now next-to-nearest-neighbor interactions are turned on, i.e., nonzero values of V_2 (and hence Y_2) are considered, the criteria of Eq. (18) remains valid in an improved form. In this case there is a need for the proper change of the scaling factor A, which now depends also explicitly on next-to-nearest-neighbor interactions. The new value of the scaling factor is

$$A(U,V_1,V_2)=\left[2\frac{z_2}{z_1}\left|\frac{2U}{z_2}+V_1+V_2\right|\right]^{-1}. \tag{19}$$

In real systems the $X_1=t_1$ requirement does not hold in general. However, the strengths of the corresponding two interactions are of the same magnitude. For $X_1\neq t_1$ only the η-pairing state of momentum $P=\pi$ represents an exact eigenstate of the model Hamiltonian H_{glob}. Figure 3 shows the stability regions of the η_π state for two different sets of model parameters expressed in units of eV in the U-t_1 plane. Dotted lines represent the boundary for stability regions corresponding to bond Hamiltonians, while solid lines are the boundaries calculated with plaquette Hamiltonians in the ab-

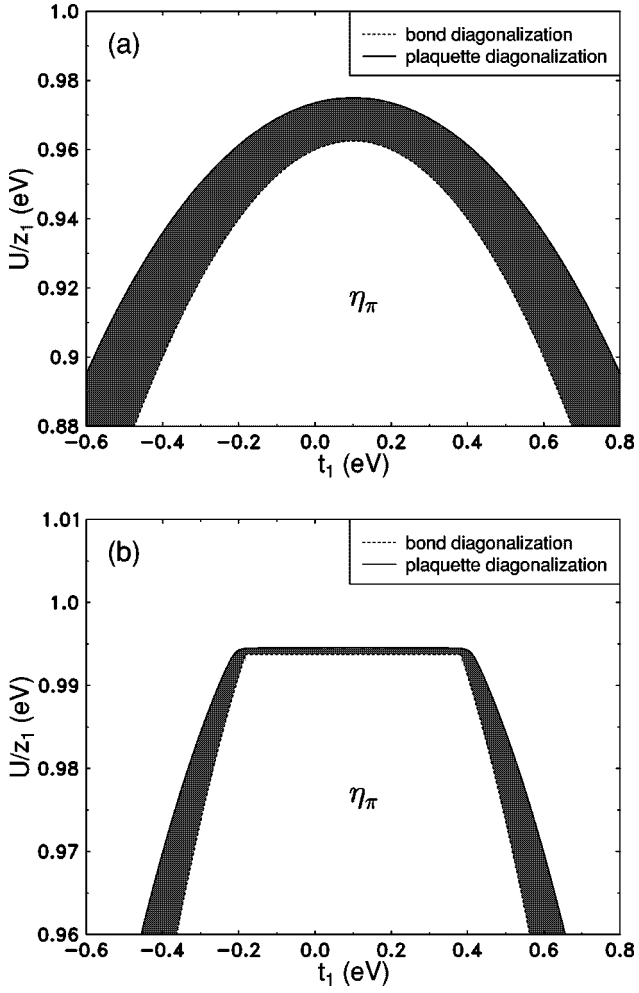

FIG. 3. Exact stability domains of η-pairing state of momentum $P=\pi$ (η_π) at half-filling for two different sets of nearest-neighbor couplings in the absence of next-to-nearest-neighbor interactions [(a) $X_1=0.1$ eV, $V_1=-2$, eV and $J_1=0.05$ eV; (b) $X_1=0.1$ eV, $V_1=-2$ eV, $J_{xy}^{(1)}=-0.02$ eV, and $J_z^{(1)}=-0.015$ eV]. The shaded regions represent the enlargement of the stability domain due to the choice of local Hamiltonian defined on plaquettes instead of bonds.

sence of next-to-nearest-neighbor interactions. The shaded regions clearly show the extension of stability regimes due to the choice of larger local Hamiltonians.

We now consider the phase diagrams in the U-Y_1 (Fig. 4) and V_2-V_1 (Fig. 5) planes for fixed values of the other interactions. In Fig. 4 the exchange interaction has been fixed by the relation $J_1=-2Y_1$. This insures that the global Hamiltonian of Sec. III coincides with the model Hamiltonian of Ref. 25, where the authors, using the method of positive semidefinite operators,[8,10,11] derived rigorous bounds for the η_π state. Comparing Fig. 4 with Fig. 1 in Ref. 25 two basic differences can be noticed. First, the boundary of the stability region, even for the special case of $X_1=t_1$, varies with increasing values of nearest-neighbor pair-hopping amplitude Y_1 and has a maximum at $Y_1\approx 1.33t_1$, instead of having a constant value. Second, the value of this maximum $U_{\max}\approx -0.33z_1t_1$ is independent of X_1. Furthermore, the stability regions for all values of X_1/t_1 derived with the present method are always larger than the corresponding ones predicted by Montorsi and Campbell[25] and de Boer and

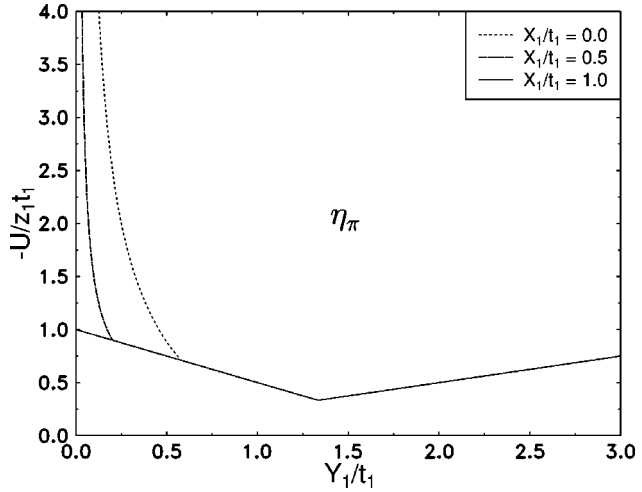

FIG. 4. Effects of correlated hopping X_1 and pair hopping Y_1 on the stability of η-pairing state of momentum $P=\pi$ (η_π). Each next-to-nearest-neighbor interaction is turned off. We note that beyond a well-defined value of Y_1 the phase boundaries for the cases $X_1\neq t_1$ and $X_1=t_1$ coincide.

Schadschneider[12] and exist for all positive values of Y_1. The relation $Y_1=-2V_1$ is also satisfied because the η_π state has to be an exact eigenstate of the model. Therefore, the positivity of Y_1 implies that the nearest-neighbor density-density type interaction V_1 has to be always negative, i.e., attractive, in order to find an η_π ground state.

As the η-pairing states consist of local pairs of electrons, it is of interest to investigate the effect of on-site Coulomb repulsion, characterized by U, on the stability of these pairs. To do this the V_2-V_1 plane is chosen at various values of U. As can be seen in Fig. 5 the local pairs are stable even in the presence of relatively large positive values of U. This requires, however, an attraction in the nearest-neighbor

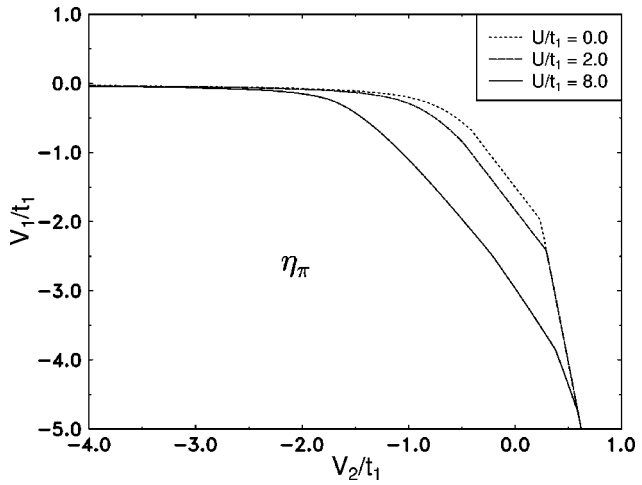

FIG. 5. Stability domains of η-pairing state of momentum $P=\pi$ (η_π) in $D=3$ in the presence of various on-site Coulomb repulsions (U) and intersite density-density type interactions (V_1,V_2). The remaining parameters of Eq. (7) are chosen as follows: $t_2=-\frac{1}{4}t_1$ and $X_1=J_1=J_2=0$. Note that X_2, Y_1, and Y_2 are uniquely fixed via the rigorous restrictions derived earlier in order that Eq. (13) be an exact eigenstate. In $D=2$ similar stability regions emerge.

density-density interaction channel. It should also be noted that the same type of interaction between next-to-nearest neighbors, denoted by V_2, can either be attractive or moderately repulsive. These findings lead us to the conclusion that the η-pairing state of momentum $P=\pi$ remains the ground states of Eq. (7) even for positive values of the on-site Coulomb interaction. Hence superconductivity can exist in the extended Hubbard model with local repulsion ($U>0$), if a sufficiently strong nearest-neighbor attraction ($V_1<0$) is present.

The inclusion of next-to-nearest-neighbor interactions increases remarkably the number of model parameters and hence the number of possible cuts of the parameter space. Therefore, we illustrate only some special, overall effects of these interactions. In order to model real systems all next-to-nearest-neighbor interactions are chosen to be smaller in magnitude than the corresponding nearest-neighbor ones. Nevertheless, the ratio of nearest to next-to-nearest-neighbor interactions can be very different—it depends on the material. In Fig. 6 three plots are shown for different values of the couplings. These belong to the case of $D=2$. The corresponding three-dimensional plots display qualitatively the same features, except for the parameters of Fig. 6(c). The quantitative discrepancy between the plots taken in $D=2$ and in $D=3$ is due to the fact that the number of next-to-nearest neighbors z_2 is much larger in $D=3$ spatial dimensions than in $D=2$ on a hypercubic lattice. This suggests that in the framework of the present model the effects of next-to-nearest-neighbor interactions are stronger in higher dimensions.

In Fig. 6(a) the stability region of the η-pairing state of momentum $P=0$ is shown for a certain set of model parameters in the absence (solid line) and in the presence (dotted line) of next-to-nearest-neighbor couplings. One can notice the expansion of the stability region due to the presence of next-to-nearest-neighbor interactions. Since a large value of $|t_1|$ (in the presence of a fixed value of the nearest-neighbor pair hopping Y_1) favors the hopping of single electrons over the hopping of electron pairs, large values of $|t_1|$ give rise to the breaking of local pairs. This means that the number of doubly occupied sites is not conserved any longer and, as a result, the η_0 state ceases to be the ground state of $H_{\rm glob}$. In Fig. 6(b) the effects of next-to-nearest-neighbor interactions on the stability of the η_π state are shown. In contrast to the situation depicted in Fig. 6(a) no shrinking of the stability domain with increasing $|t_1|$ can be observed. This can be explained with the different internal structure of the η_π pairs. In Fig. 6(c) we show a situation, where next-to-nearest-neighbor couplings can either extend or shrink the stability region of the η_π state. As mentioned earlier, the dimension of the lattice plays a crucial role here. In $D=2$ a huge portion of the U-Y_1 plane phase diagram is occupied by the η_π state for any ratio of X_1/t_1. In $D=3$, however, it was found for a wide parameter region that the η_π-state is the ground state of the model Hamiltonian $H_{\rm glob}$ only for the special case of $X_1/t_1=1$.

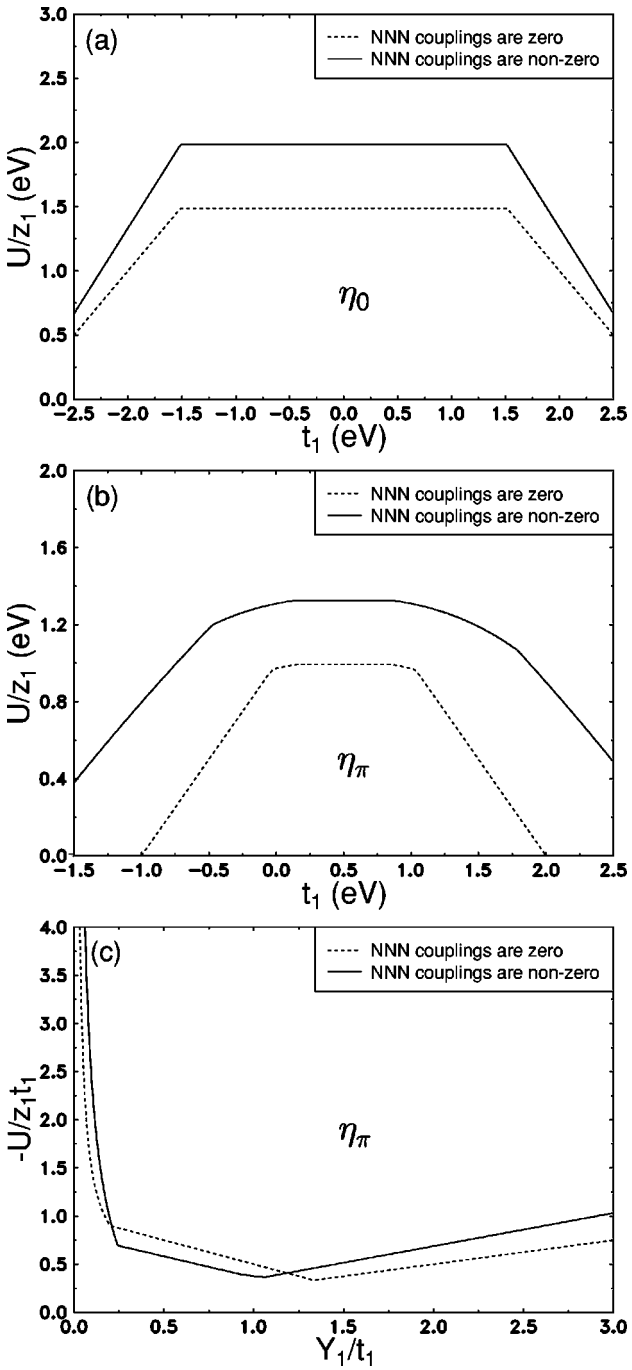

FIG. 6. Effects of next-to-nearest-neighbor (NNN) couplings on the stability of η-pairing states of momentum P on a two-dimensional square lattice. The values of the interaction constants are fixed as follows: (a) $P=0$, $V_1=-3$ eV, $J_{\rm xy}^{(1)}=\frac{1}{40}$ eV, $J_{\rm z}^{(1)}=\frac{1}{30}$ eV, $t_2=\frac{1}{3}t_1$, $V_2=\frac{1}{3}V_1$, and $J_{\rm a}^{(2)}=\frac{1}{3}J_{\rm a}^{(1)}$ ($a=xy,z$); (b) $P=\pi$, $V_1=-2$ eV, $X_1=0.5$ eV, $J_{\rm xy}^{(1)}=-\frac{1}{50}$ eV, $J_{\rm z}^{(1)}=-\frac{1}{40}$ eV, $t_2=-\frac{1}{3}t_1$, $V_2=\frac{1}{3}V_1$, and $J_{\rm a}^{(2)}=\frac{1}{3}J_{\rm a}^{(1)}$ ($a=xy,z$); (c) $P=\pi$, $X_1=\frac{1}{2}t_1$, $J_1=-2Y_1$, $t_2=-\frac{1}{5}t_1$, $Y_2=\frac{1}{8}Y_1$, and $J_2=\frac{1}{8}J_1$.

B. Fully polarized ferromagnetic state

Let us consider now the fully (z-) polarized ferromagnetic state as the trial wave function defined as

$$|\Psi_{\rm FM}\rangle=\prod_{j=1}^{L} c_{j\uparrow}^{\dagger}|0\rangle=\hat{F}|0\rangle. \tag{20}$$

Calculating the commutator of $\hat{F}$ with $H_{\rm glob}$ one can see that this state is an exact eigenstate of the global Hamiltonian for any values of the interaction parameters. The trial wave func-

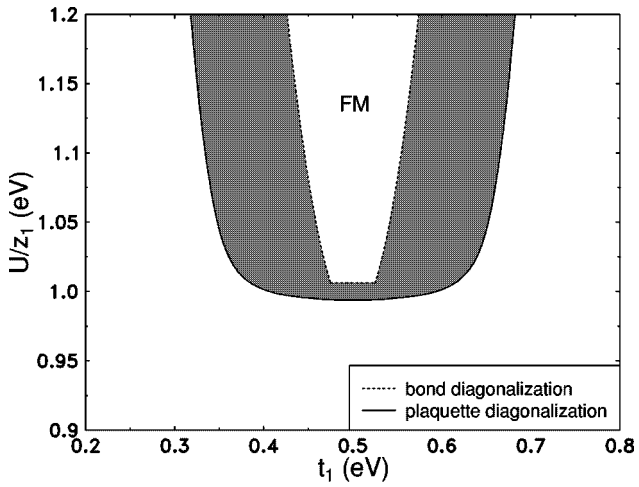

FIG. 7. Exact stability region for the fully saturated ferromagnetic (FM) state at half-filling on a D-dimensional hypercubic lattice for a certain set of model parameters $X_1=0.5$ eV, $V_1=2$ eV, and $Y_1=-J_1=\frac{1}{40}$ eV in the absence of next-to-nearest-neighbor interactions. The shaded region represents the extension of the stability of the fully saturated ferromagnetic state as the ground state of Eq. (7) due to the choice of local Hamiltonian defined on elementary plaquettes, instead of bonds, of the lattice.

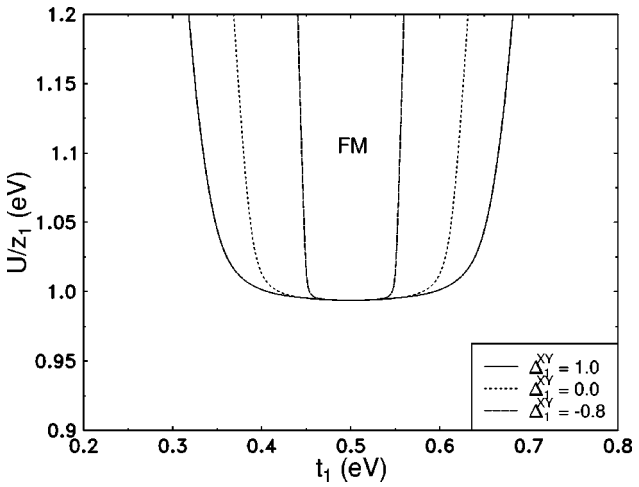

FIG. 8. Stability regions of the fully saturated FM state for various values of Δ_1^{XY}. The stability region is maximal at $\Delta_1^{XY}=1$ and vanishes for values $\Delta_1^{XY}<-1$. The numerical values of the remaining couplings are the same as in Fig. 7.

tion $|\Psi_{\mathrm{FM}}\rangle$ yields in the thermodynamic limit at half-filling the upper bound

$$E_{\mathrm{upper}}^{\mathrm{FM}}=-\tfrac{1}{4}UL+\tfrac{1}{8}L\sum_{l=1}^{2}z_l J_{\mathrm{z}}^{(l)}-\mu L \tag{21}$$

for the ground-state energy.

In what follows, we reveal under what conditions Eq. (20) is the ground state of H_{glob}. For the sake of simplicity we concentrate on a fixed set of numerical values of nearest-neighbor couplings, as it has already been estimated by Hubbard[28] for electrons in d bands of transition metals. The values of next-to-nearest-neighbor interactions are chosen to be fractions of the corresponding nearest-neighbor ones. The ratio of nearest- to next-to-nearest-neighbor couplings is set to be approximately 5–8. We consider this range of ratio to be appropriate for a wide class of materials. Furthermore, this is in agreement with the work of Appel, Grodzicki, and Paulsen,[29] who also made quantitative predictions regarding the strength of nearest- and next-to-nearest-neighbor correlated hopping X_1 and X_2, respectively. Further calculations at different sets of model parameters have also shown that the phase diagrams plotted in Figs. 7, 8, and 9 are generic. This suggests that the above choice of model parameters captures the essential physics.

In Fig. 7 we present the changes in the stability domain induced by using plaquette Hamiltonians. For comparison with the corresponding result of Ref. 12 with bond Hamiltonians, the plaquette Hamiltonians contained no next-to-nearest-neighbor interactions. The shaded region shows the enlargement in the stability domain of the fully saturated ferromagnetic state. As can be seen from the figure, there is a reasonable extension with respect to t_1. While in the case of bond Hamiltonians the value of the correlated hopping X_1 should be very close in magnitude to t_1 in order to reach the boundary of the stability region at $U_{\mathrm{min}}\approx 4$ eV, we have a much broader region for that using plaquette Hamiltonians. The broadening implies that the additionally incorporated spatial correlations really lead to the stabilization of the ordered phase, in our case the ferromagnetism.

The global Hamiltonian H_{glob} containing purely nearest-neighbor interactions can be transformed into an effective Heisenberg model in the large-U limit at half-filling (see, e.g., Vollhardt *et al.*[30] and references therein) with the effective exchange coupling of

$$J_{\mathrm{eff}}=\frac{t_1^2}{U}\left(1-\frac{X_1}{t_1}\right)^2+J_1. \tag{22}$$

This favors ferromagnetism for all $J_{\mathrm{eff}}<0$. Neglecting in Eq. (7) all intersite interactions but the nearest-neighbor exchange interaction, the latter equation suggests a simple perturbative criterion for the stability of ferromagnetism in the large-U limit; ferromagnetism is favored over antiferromagnetism for all $U>U_{\mathrm{c}}=t_1^2/|J_1|$ (note that in Eq. (7) $J_1=-|J_1|<0$ means the ferromagnetic coupling). It is known that the OGS approach using bond Hamiltonians gives the criterion $U/z_1>U_{\mathrm{c}}$ as the stability requirement in the same regime. Therefore it possibly underestimates the stability of the fully polarized ferromagnetic state. Taking into account larger local Hamiltonians defined on elementary plaquettes of the hypercubic lattice one gets the criterion $U/z_1>U_{\mathrm{c}}/2$ for the stability, which means more extended stability domain in the large-U limit. Furthermore, it suggests that (at least in the large-U limit) the stability criterion has the form of $U>(z_1/b)U_{\mathrm{c}}$, where b is the function of the size of the cluster on which the local Hamiltonian is defined. The possible scaling behavior of the stability criterion and the concrete form of $b(N_{\mathrm{cluster}})$ are discussed elsewhere.[31]

Since the fully polarized ferromagnetic state at half-filling is an exact eigenstate of H_{glob} we have got no *a priori* restrictions for the values of the interaction parameters. The extensive calculations, however, lead to a simple restriction between $J_{\mathrm{xy}}^{(1)}$ and $J_{\mathrm{z}}^{(1)}$. In order to have a ferromagnetic ground state of a model containing spin interactions that vary continuously from a Heisenberg-type interaction to a simple

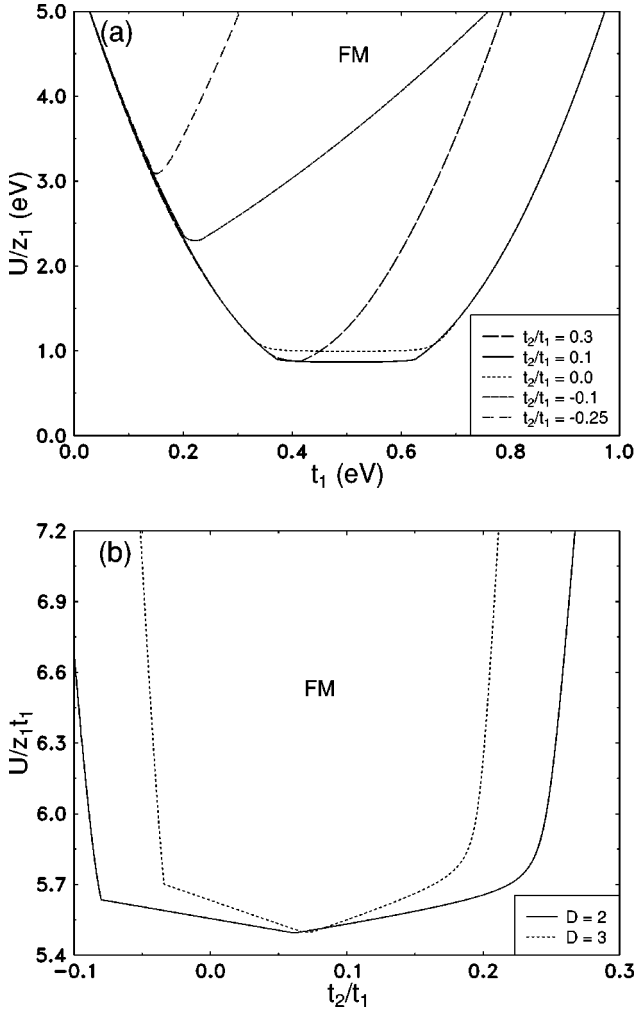

FIG. 9. Effects of next-to-nearest-neighbor couplings on the stability of the fully saturated FM state at half-filling in the t_1-U and t_2-U planes, (a) and (b), respectively. (a) shows the phase boundaries for various ratios of t_2/t_1 choosing the numerical values of nearest-neighbor interactions as in Fig. 7. Next-to-nearest-neighbor interactions for the plot are as follows: $X_2=0.08$ eV, $V_2=\frac{1}{8}V_1$, $Y_2=\frac{1}{5}Y_1$, and $J_2=\frac{1}{5}J_1$. In (b) all the interaction constants are expressed in units of t_1 instead of units of eV. Above each line the ground state is the fully polarized ferromagnetic state.

Ising-type one, the $-1<\Delta_1^{XY}\leqslant 1$ requirement must hold. This means that the restriction

$$-|J_z^{(1)}|\leqslant -J_{xy}^{(1)}<|J_z^{(1)}| \tag{23}$$

has to be always satisfied. In Fig. 8 the consequence of Eq. (23) is illustrated in the U-t_1 cut of the parameter space at $\Delta_1^Z=1$ and $J_z^{(1)}=-|J_z^{(1)}|<0$ for various values of Δ_1^{XY}. The size of the stability region is maximal at $\Delta_1^{XY}=1$ and gradually decreases as Δ_1^{XY} reaches $\Delta_1^{XY}=-1$. Any further decrease of Δ_1^{XY} yields that our ferromagnetic state that is fully z polarized is no longer the ground state of $H_{\rm glob}$; for $J_{xy}^{(1)}=J_z^{(1)}$ $H_{\rm glob}$ is SU(2) symmetric, which implies the degeneracy of the ground state with respect to SU(2) rotations. For anisotropic exchange couplings favoring the xy plane, the ground-state polarization may still be macroscopic, however, it no longer points in the z direction. This means that the fully z-polarized ferromagnetic trial wave function becomes unstable. We note that Eq. (23) must hold even in the presence of next-to-nearest-neighbor couplings.

In Fig. 9 the effects of nonzero next-to-nearest-neighbor hopping t_2 are illustrated for a fixed set of model parameters, first in the U-t_1 plane [(a), in units of eV] and second in the U-t_2 plane [(b), in units of t_1]. In Fig. 9(a) the dotted line represents the phase boundary in the absence of next-to-nearest-neighbor interactions while solid, long-dashed, dashed, and dotted-dashed lines correspond to phase boundaries in the presence of next-to-nearest-neighbor interactions for various values of t_2. As can be seen from the plot, next-to-nearest-neighbor interactions can help in stabilizing ferromagnetism for the chosen set of model parameters as long as t_2/t_1 has a small, positive value. For negative or large positive values of t_2/t_1, however, the stability domain reduces significantly and stronger Coulomb repulsion is needed for the stabilization. This means, e.g., that for a reasonably narrow band ($t_1\approx 0.4$ eV) with the ratio of $t_2/t_1=0.1$, the required minimal stabilizing Coulomb repulsion is about $U_{\rm min}\approx 3$ eV. The same value of U at $t_2/t_1=-0.25$ is about $U_{\rm min}\approx 30$ eV, which is a magnitude larger. Nevertheless, the above range of Coulomb interactions can be considered reasonable for real materials.

In Fig. 9(b) the effects of change in non-interacting dispersion due to the inclusion of next-to-nearest-neighbor hopping are shown for a square (solid line) and for a cubic (dotted line) lattice. The stability domains of ferromagnetism depend on the dimensionality of the lattice and do not coincide. It is interesting to note that the most favorable values of t_2/t_1 for which the Coulomb interaction takes its minimal value $U_{\rm min}$ also depend on the spatial dimension. The shapes of the stability domains are also of interest: in a well-defined region of t_2/t_1 $U_{\rm min}$ changes only by a slight amount but as soon as the edges of this region are reached U increases drastically. This feature suggests that inside the stability regions a nonzero next-to-nearest-neighbor hopping via the asymmetric density of states[13,32] helps (in the presence of other next-to-nearest-neighbor interactions) in stabilizing ferromagnetism but outside it destabilizes ferromagnetic ordering. The edges are determined mainly by the dispersions (hence the shape of the particular density of states) and tuned further by other interactions being present in $H_{\rm glob}$.

It is also known that the inclusion of nearest-neighbor ferromagnetic exchange interaction in the pure Hubbard model favors the parallel ordering of electron spins.[4,11,19] In Fig. 10 we considered the pure Hubbard model supplemented with next-to-nearest-neighbor hopping t_2 and nearest- and next-to-nearest-neighbor exchange interactions J_1 and J_2, respectively. All the other type of couplings are turned off. As can be seen in the figure, the stability domain of ferromagnetism extends with increasing value of the Coulomb repulsion and in the limit of $U\to\infty$ fills the whole $J_1, J_2\leqslant 0$ quarter of the phase diagram. The fully polarized ferromagnetic state remains the ground state of Eq. (7) for finite values of U only in the presence of finite values of J_1 and J_2. Figure 10 also shows that the required minimal values of $|J_2|$ are about an order of magnitude less than the

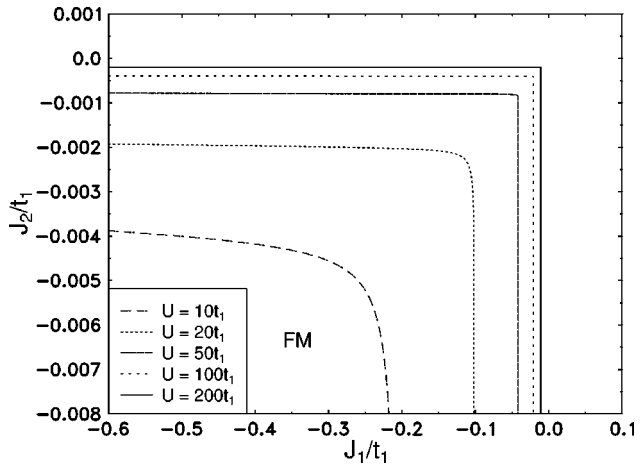

FIG. 10. Stability of the fully saturated FM state in the presence of nearest (J_1) and next-to-nearest (J_2) -neighbor exchange coupling at $t_2=-\frac{1}{10}t_1$. All the other interactions are turned off, i.e., $X_1=X_2=V_1=V_2=Y_1=Y_2=0$.

required minimal values of $|J_1|$, and J_2 should also be ferromagnetic in nature, i.e., $J_2<0$.

V. CONCLUSIONS

In the present paper we have studied in the thermodynamic limit the ground-state phase diagram of the Hubbard model supplemented by nearest- and next-to-nearest-neighbor interactions. The purpose of the study was to clarify to what extent and in which way the inclusion of additional spatial correlations changes the stability of physically interesting states, the η-pairing state of momentum $P=0$ and $P=\pi$, or the fully z-polarized ferromagnetic state. The phase boundaries are extracted from the equality of an upper and a lower bound of the ground-state energy, hence these are exact. The additional spatial correlations are introduced via the computation of the lower bound on elementary plaquettes, instead of bonds, of the D-dimensional hypercubic lattice. Except the case of η-pairing state of momentum $P=0$ the exact phase boundaries cannot be given in closed, analytic forms. Instead, they are shown graphically in special cuts of the parameter space of the model under study.

The phase boundaries presented are *sufficient* phase boundaries. This means that outside the region defined by the exact conditions a certain state might remain the ground state of the model. Diagonalizing local Hamiltonians defined on larger clusters of the lattice the phase boundaries might be further improved. This improvement with increasing cluster size addresses a further issue: does the stability domain of a given ordered phase extend further with taking larger and larger clusters, or is there a convergence regarding the location of its phase boundary? If the latter holds, we could determine the phase boundaries with a simple extrapolation even in the limit of $H=h_{\text{cluster}}$. Based on preliminary results we believe that the further extension of stability domains decreases rapidly with increasing cluster size. For instance, computing the lower bounds of the ground-state energy with diagonalizing local Hamiltonians defined on clusters of six lattice sites, the further expansion of the stability regions is only a few percent, generally 4–5 % or less.

Considering the effects of more spatial correlations, which was equivalent in our case with the choice of plaquette Hamiltonians, we have improved significantly the previously derived rigorous results of Refs. 11,12,24,25. This means, e.g., for the fully polarized ferromagnetic state that the minimal value of the Coulomb repulsion required to stabilize ferromagnetism along reasonable values of nearest-neighbor interactions is predicted to be about 6–10 eV (in $D=3$) in a relatively broad range of nearest-neighbor hopping (see Fig. 7).

Another goal of the present study was to determine the overall effects of next-to-nearest-neighbor interactions on the stability domains. The inclusion of next-to-nearest-neighbor interactions can be done naturally using plaquette Hamiltonians. To our knowledge, the effects of next-to-nearest-neighbor interactions, except those of next-to-nearest-neighbor hopping, have not yet been considered rigorously in the literature. The relative strengths of next-to-nearest-neighbor interactions are much smaller than that of nearest-neighbor interactions, the stability conditions, however, strongly depend on them. Their effect in various sectors of the phase diagram is different and they result either an extension or a shrinking of the stability domain. For instance, taking the η-pairing state of momentum $P=\pi$ the possible maximal value of the Coulomb repulsion $U_{\max}$, up to which the η_π state remains the ground state of the extended Hubbard model (i.e., the model has a superconducting ground state), is increased from 6 to 8–9 eV (in $D=3$) by the inclusion of relatively small next-to-nearest-neighbor interactions [Fig. 6(b)].

It is also known that next-to-nearest-neighbor hopping of single particles, which is characterized by the hopping amplitude t_2, is of importance in real materials. Our results are in good agreement with this fact. We showed that t_2 has a characteristic effect, e.g., on the stability of the fully saturated ferromagnetic state. Even a small ratio of t_2/t_1, i.e., a small amount of frustration in the dispersion, introduces a qualitative change into the phase diagram. The change is mostly a shrinking of the stability domain, however, for small ratios ($t_2/t_1\leqslant 0.15$) the presence of t_2 helps in stabilizing ferromagnetism (Fig. 9). This is in good agreement with recent DMRG studies made on a one-dimensional triangular lattice.[33] It is interesting to note that in our calculations the extension of ferromagnetic domain occurs always at positive ratios of t_2/t_1 for fixed values of the other parameters of the model.

The Hubbard model supplemented only by exchange interactions J_1 and J_2 has also been investigated. Our results are in good agreement with Ref. 34, i.e., the critical values of nearest- and next-to-nearest exchange interactions to give rise to ferromagnetism approach zero as $U\rightarrow\infty$ in the case of a half-filled band in any dimensions. However, at finite values of the Coloumb repulsion J_1 and J_2 should also be finite, if the ground state is the fully polarized ferromagnetic state.

In summary, we have established a simple method that allows us to incorporate and to treat the effects of next-to-nearest-neighbor correlations and interactions in an *exact* fashion. We showed that the ground state of the extended Hubbard model in the thermodynammic limit at half-filling is superconducting or ferromagnetic, depending on the inter-

action strengths. The improved phase boundaries for certain sets of model parameters have also been constructed.

ACKNOWLEDGMENTS

The author would like to thank Zs. Gulácsi and E. Müller-Hartmann for their continuous encouragement during the present work. He also thanks A. Schadschneider, F. Pázmándi, G. Uhrig, and P. Wurth for valuable discussions and careful reading of the manuscript. The author gratefully acknowledges financial support of Deutscher Akademischer Austauschdienst (DAAD) and the hospitality of the University of Cologne, Germany.

*Permanent address: Danubia Patent & Trademark Attorneys Ltd., H-1368 Budapest 5, POB 198, Hungary.

[1] E. H. Lieb and F. Y. Wu, Phys. Rev. Lett. **20**, 1445 (1968).
[2] W. Metzner and D. Vollhardt, Phys. Rev. Lett. **62**, 324 (1989).
[3] E. Müller-Hartmann, Z. Phys. B **74**, 507 (1989); **76**, 211 (1989).
[4] J. C. Amadon and J. E. Hirsch, Phys. Rev. B **54**, 6364 (1996).
[5] M. Ulmke, Eur. Phys. J. B **1**, 301 (1998).
[6] F. H. L. Essler, V. E. Korepin, and K. Schoutens, Phys. Rev. Lett. **70**, 73 (1993).
[7] A. A. Ovchinnikov, J. Phys.: Condens. Matter **6**, 11 057 (1994).
[8] U. Brandt and A. Giesekus, Phys. Rev. Lett. **68**, 2648 (1992).
[9] A. Mielke and H. Tasaki, Commun. Math. Phys. **158**, 341 (1993).
[10] R. Strack and D. Vollhardt, Phys. Rev. Lett. **70**, 2637 (1993).
[11] R. Strack and D. Vollhardt, Phys. Rev. Lett. **72**, 3425 (1994).
[12] J. de Boer and A. Schadschneider, Phys. Rev. Lett. **75**, 4298 (1995).
[13] T. Hanisch, G. S. Uhrig, and E. Müller-Hartmann, Phys. Rev. B **56**, 13 960 (1997).
[14] H. Tasaki, Phys. Rev. Lett. **75**, 4678 (1995).
[15] R. Hlubina, S. Sorella, and R. Guinea, Phys. Rev. Lett. **78**, 1343 (1997).
[16] C. Verdozzi and M. Cini, Phys. Rev. B **51**, 7412 (1995).
[17] J. van den Brink *et al.*, Phys. Rev. Lett. **75**, 4658 (1995).
[18] Zs. Szabó and Zs. Gulácsi, Philos. Mag. B **76**, 911 (1997).
[19] J. E. Hirsch, Phys. Rev. B **56**, 11 022 (1997).
[20] M. Kollar, R. Strack, and D. Vollhardt, Phys. Rev. B **53**, 9225 (1996).
[21] J. de Boer, V. E. Korepin, and A. Schadschneider, Phys. Rev. Lett. **74**, 789 (1995).
[22] A. Montorsi and D. K. Campbell, Phys. Rev. B **53**, 5153 (1996).
[23] C. N. Yang, Rev. Mod. Phys. **34**, 694 (1962).
[24] C. N. Yang, Phys. Rev. Lett. **63**, 2144 (1989).
[25] S.-Q. Shen and Z.-M. Qiu, Phys. Rev. Lett. **71**, 4238 (1993).
[26] A. A. Aligia and L. Arrachea, Phys. Rev. Lett. **73**, 2240 (1994).
[27] A. Schadschneider, Phys. Rev. B **51**, 10 386 (1995).
[28] J. Hubbard, Proc. R. Soc. London, Ser. A **276**, 238 (1963).
[29] J. Appel, M. Grodzicki, and F. Paulsen, Phys. Rev. B **47**, 2812 (1993).
[30] D. Vollhardt *et al.*, Z. Phys. B **103**, 283 (1997).
[31] Zs. Szabó (unpublished).
[32] J. Wahle *et al.*, Phys. Rev. B **58**, 12 749 (1998).
[33] R. Arita, Y. Shimoi, K. Kuroki, and H. Aoki, Phys. Rev. B **57**, 10 609 (1998).
[34] J. E. Hirsch, J. Appl. Phys. **67**, 4549 (1990).